Published in final edited form as:

Cancer. 2018 March 01; 124(5): 1008–1015. doi:10.1002/cncr.31173.

Bone Biopsy Protocol for Advanced Prostate Cancer in the Era of Precision Medicine

Verena Sailer, MD[1,2], **Marc H Schiffman, MD**[4], **Myriam Kossai, MD**[1,2], **Joanna Cyrta, MD**[1,2], **Shaham Beg, MD**[1,2], **Brian Sullivan**[4], **Bradley B Pua, MD**[4], **Kyungmouk Steve Lee, MD**[4], **Adam D. Talenfeld, MD**[4], **David M Nanus, MD**[3,5], **Scott T Tagawa, MD**[3,5], **Brian D. Robinson, MD**[1,2], **Rema A. Rao, MD**[1,2], **Chantal Pauli, MD**[1,2], **Rohan Bareja**[2,6], **Luis S. Beltran, MD**[7], **Alexandros Sigaras, MS**[2], **Kenneth Wa Eng, MS**[2,3,8], **Olivier Elemento, PhD**[1,2,6,8], **Andrea Sboner, PhD**[1,2,6], **Mark A. Rubin, MD**[1,2,3], **Himisha Beltran, MD**[2,3,5,#], and **Juan Miguel Mosquera, MD, MSc**[1,2,#]

[1]Department of Pathology and Laboratory Medicine, Weill Cornell Medicine, New York, NY, USA

[2]Caryl and Israel Englander Institute for Precision Medicine, Weill Cornell Medicine and New York Presbyterian, New York, NY, USA

[3]Sandra and Edward Meyer Cancer Center, Weill Cornell Medicine and New York Presbyterian, New York, NY, USA

[4]Department of Radiology, Weill Cornell Medicine, New York, NY, USA

[5]Department of Medicine, Division of Hematology and Medical Oncology, Weill Cornell Medicine, New York, NY, USA

[6]Institute for Computational Biomedicine, Weill Cornell Medicine, New York, NY, USA

[7]Department of Radiology, NYU Langone Medical Center, New York, NY, USA

[8]Department of Physiology and Biophysics, Weill Cornell Medicine, New York, NY, USA

Abstract

Corresponding authors: Juan Miguel Mosquera, MD, MSc, Department of Pathology and Laboratory Medicine, Weill Cornell Medicine, 1300 York Avenue, Box 69, New York, NY, 10065, USA, Phone: (212) 746-2700, Fax: (212) 746-8624, jmm9018@med.cornell.edu; Himisha Beltran, MD, Division of Medical Oncology, Weill Cornell Medicine, 413 East 69th Street, 14th floor, New York, NY 10021, Phone: (646) 962 2072, Fax: (646) 962 1603, hip9004@med.cornell.edu.
[#]These authors share senior authorship

Author contributions: Verena Sailer: Conceptualization, tissue processing and histopathological review, methodology, formal analysis, data curation, writing-original draft, writing-review. **Marc H Schiffmann:** Performed biopsy procedures, data curation, writing-original draft. **Myriam Kossai:** Tissue processing and histopathological review, data curation. **Joanna Cyrta:** Tissue processing and histopathological review, data curation. **Shaham Beg:** Tissue processing and histopathological review, data curation. **Brian Sullivan:** Performed biopsy procedures. **Bradley B Pua:** Performed biopsy procedures. **Kyungmouk Steve Lee:** Performed biopsy procedures. **Adam D. Talenfeld:** Performed biopsy procedures. **David M Nanus:** Investigation, patient consent. **Scott T Tagawa:** Investigation, patient consent. **Brian D. Robinson:** Tissue processing and histopathological review. **Rema A. Rao:** Tissue processing and histopathological review. **Chantal Pauli:** Tissue processing and histopathological review, data curation. **Rohan Bareja:** Data analysis. **Luis S. Beltran:** Performed radiographic procedure and analysis. **Alexandros Sigaras:** Data analysis. **Kenneth Wa Eng:** Data analysis. **Olivier Elemento:** Data analysis. **Andrea Sboner:** Data analysis. **Mark A. Rubin:** Conceptualization, funding acquisition, writing-review. **Himisha Beltran:** Conceptualization, investigation, funding acquisition, patient consent, writing-original draft. **Juan Miguel Mosquera:** Conceptualization, supervision, funding acquisition, writing-original draft.

Conflict of interest disclosures: The authors declare no conflicts of interest.

Background—Metastatic biopsies are increasingly being performed in patients with advanced prostate cancer to look for actionable targets and/or identify emerging resistance mechanisms. Due to a predominance of bone metastases and their sclerotic nature, obtaining sufficient tissue for clinical and genomic studies is challenging.

Methods—Patients with prostate cancer bone metastases were enrolled between February 2013 and March 2017 on an IRB-approved protocol for prospective image-guided bone biopsy. Bone biopsies and blood clots were collected fresh. Compact bone was subjected to formalin with a decalcifying agent for diagnosis; marrow and blood clots were frozen in optimum cutting temperature (OCT) formulation for NGS. Frozen slides were cut from OCT cryomolds and evaluated for tumor histology and purity. Tissue was macrodissected for DNA and RNA extraction, and whole-exome sequencing (WES) and RNA-seq were performed.

Results—Seventy bone biopsies from 64 patients were performed. Diagnostic material confirming prostate cancer was successful in 60/70 (85.7%) cases. Median DNA/RNA yield was 25.5 ng/μl and 16.2 ng/μl, respectively. WES was performed successfully in 49/60 (81.7%) of patients, with additional RNA-seq in 20/60 (33.3%). Recurrent alterations were as expected including those involving the *AR*, *PTEN*, *TP53*, *BRCA2*, and *SPOP* genes.

Conclusion—This prostate cancer bone biopsy protocol ensures a valuable source for high quality DNA and RNA for tumor sequencing and may be used to detect actionable alterations and resistance mechanisms in patients with bone metastases.

Keywords

Bone metastases; Biopsy; DNA; NGS; Prostate cancer; Precision Medicine; RNA

Introduction

Ninety percent of patients with metastatic prostate cancer harbor bone metastases and up to 42.9% of patients have bone-only metastases [1, 2] With an estimated 26,730 patients succumbing to their disease in 2017 in the United States alone,[3] prostate cancer and associated bone metastases represent a large health burden worldwide.

The therapeutic portfolio for patients with metastatic prostate cancer is evolving based on an improved understanding of the molecular framework of metastatic prostate cancer and the identification of potentially actionable targets enriched in advanced disease (e.g., homologous recombination genomic alterations and PARP inhibitors; mismatch repair/microsatellite instability and immunotherapy).[4, 5] Biomarker and genomic studies in prostate cancer have been predominantly based on metastatic biopsy protocols embedded within clinical trials and/or developed through consortium efforts at specialized centers including the Stand Up To Cancer-Prostate Cancer Foundation Dream Teams.[4-6]

Sclerotic bone lesions have been notoriously challenging to biopsy, the amount of tissue obtained being scant and requiring decalcification, often inadequate for extensive molecular analyses.[7, 8] Using an unguided approach, a previous study demonstrated, that only 25.5% of 184 patients with metastatic prostate cancer had a positive bone biopsy [19]. Although success rates for image-guided bone biopsies in specialized academic centers have significantly

improved in recent years, broader application of bone biopsy protocols across the clinical community is challenged by a lack of standardized protocols.

Here we provide a detailed description of a successful next-generation biopsy protocol amenable to sclerotic bone lesions of advanced prostate cancer patients and broadly applicable to the clinical community. We combine clinical and radiographic features, image-guided percutaneous techniques, and standardized pathology processing protocols to optimize the yield and quality of tissues obtained for downstream testing.

Methods

Patient cohort

Patients with metastatic prostate cancer were prospectively enrolled on an ongoing Precision Medicine clinical trial at Weill Cornell Medicine from February 2013 until March 2017 and underwent image-guided bone biopsy by Interventional Radiology.[9] IRB-approved written consent was obtained prior to metastatic biopsy, genomic testing, and clinical follow-up. All lesions were reviewed prospectively by one Interventional Radiologist (MHS), and were defined as sclerotic, mixed or lytic via qualitative comparison of attenuation with adjacent areas of intact cortical bone. A schematic figure of the workflow and specimen images can be found in Figure 1 and Figure 2.

CT-guided bone biopsy

To identify the shortest path to the bone lesion without intervening vital structures, a biopsy plan was developed based on pre-procedure review of standard computed tomography (CT) and bone scan images. The procedure image was reviewed to ensure targeting of metabolic lesions on the nuclear scans, and progressing lesions, if seen, were preferentially biopsied. The plan for each case was to acquire as many cores and large blood clots as safely possible. The shortest path from the skin to the lesion was drawn, attempting to target the periphery of the lesion for the initial cores in sclerotic lesions, or through and through the lesions including the near and far periphery for smaller lesions. Any area was targeted in lytic/mixed lesions. Multiple cores were planned for each case, with the bony yield determining the ultimate number taken. Patients were placed on the CT gantry (Optima CT-580 16 slice wide-bore scanner, GE Healthcare Little Chalfont, UK) in supine, prone or decubitus positions allowing for the selected path and patient comfort. Focal scout images through the target region were performed with 5mm slices and the patients were prepped in usual sterile fashion. The skin and periosteum overlying the designated biopsy area were anesthetized with 1% lidocaine (Hospira Inc, Lake Forest, IL, USA). Patients received IV conscious sedation with midazolam and fentanyl, administered and monitored by independent nursing supervision. Biopsies were taken under serial CT-guidance (Figure 3). The following biopsy systems were used for tissue procurement: Arrow® OnControl® Coaxial Powered Bone Marrow Biopsy System (Teleflex, Morrisville, NC, USA), Temno Evolution™ Biopsy Device (Bauer, Via del Fosso, Italy), Westcott Fine Needle Aspiration Biopsy (Becton Dickinson, Franklin Lakes, NJ, USA), MADISON™ Comprehensive Bone Biopsy System (Laurane Medical, Westbrook, CT, USA). After each core, aspirates were obtained and allowed to start to clot (Arrow® OnControl® only), and large clots were placed on telfa pad

to be frozen. Bleeding back through the large gauge introducer was allowed, with this material used to gather clot as well. Bone biopsies and aspiration samples were handed to the assistant who immediately placed them on top of wet ice. The biopsy needles were removed and sterile dressings were applied. Post procedure images were taken routinely to exclude immediate complications and patients were brought to the recovery area.

Biobanking and tissue processing of bone biopsies

Bone cores and blood clots were immediately transported on wet ice to the pathology department and tissue was allocated on-site for clinical diagnosis, whole exome sequencing (WES), RNA-seq, and organoid development (Figure 1). Tissue was submitted for organoid development only if concurrent cytology smear was positive for tumor (Figure 2).[28] If it was negative, tissue destined for organoid development was instead frozen for subsequent NGS, if sufficient tumor cells were present at review of frozen slides. Cores were separated into bone marrow and cortical bone. The latter was submitted for clinical diagnosis following standard decalcification. Both bone marrow and blood clots were snap frozen in O.C.T compound (Tissue-Tek®, Sakura Finetek USA Inc., Torrance, CA, USA). Frozen sections were cut from the cryomolds and stained with hematoxylin/eosin (H&E). Clinical (*i.e.* cortical bone) and research/precision medicine (*i.e.* frozen marrow and blood clots) H&E slides were reviewed by a board-certified pathologist. The frozen H&E slides were also included during the standard of care review process. A standard of care report was issued for the cortical bone (clinical) specimen. If the clinical specimen was negative for carcinoma, the tissue on the cryomolds was converted into formalin-fixed paraffin-embedded tissue (FFPE) for clinical purposes. H&E frozen section slides of bone marrow and/or blood clots were always reviewed for tumor adequacy and tumor quantification before sequencing, and compared with the corresponding clinical material (*i.e.* decalcified cortical bone). Both FFPE tissue slides (surgical pathology clinical slides) and frozen section slides (Precision Medicine clinical trial slides) were scanned at high-definition (svs file format) using the Aperio AT2 system (Leica Biosystems, Nussloch, Germany) into e-Slide manager, a password protected online platform hosted by the Information, Technologies and Service (ITS) department at Weill Cornell Medicine. These images are integrated in the WES report (for a WES/RNA report example and standard operating procedures (SOP) see Supplementary Information).

High density tumor areas were annotated on the H&E-stained glass slide by the pathologist, and tumor cell content was estimated. A published morphologic classification of metastatic prostate cancer was applied to annotate histology.[10] Tumor areas on cryomolds were sampled with a 1.5mm biopsy punch using the annotated H&E as guide. DNA and RNA extraction was performed as previously described.[9] DNA concentration was measured by the Qubit™ Fluorometric Quantitation system in ng/μl (ThermoFisher Scientific, Waltham, MA, USA) and NanoDrop (NanoDrop Technologies, Wilmington, DE, USA).[11] NanoDrop was also used for RNA concentration and nucleic acids purity (wavelenght absorption at 260/280nm). Germline DNA from blood or buccal swabs served as control.[9] Subsequent WES/RNA-seq and computational analysis were performed as described in detail before.[9] Our custom computational pipeline includes clonality analysis and sample matching check by CLONET and SPIA, respectively.[12, 13]

Statistical analysis

Comparison between groups was performed using the Fisher's exact test, T-Test and the one-way analysis of variance (one-way ANOVA). Data collection and analysis was performed with the IBM SPSS Statistics, Version 24.0 (IBM Corporation, Armonk, NY, USA). P-values lower than 0.05 were considered significant.

Results

Demographic and radiologic characteristics

Median patient age at time of consent was 71 years (range: 51-92 years). Seventy bone biopsies from 64 patients were performed; of these, 49 (70%) biopsies yielded both bone cores and blood clots simultaneously. Bone biopsies were obtained in 63/70 cases and blood clots were acquired in 56/70 cases. The number of bone biopsy cores ranged from one core up to eight cores. Blood clots only were obtained in 7/70 cases (Table 1, Clinical and pathological characteristics of 70 bone metastases from 64 patients). Sixty-one (87.1%) of bone biopsies were from sclerotic (blastic) lesions, 8 (11.4%) from lytic lesions and one lesion (1.4%) was mixed blastic/lytic. Biopsy sites were iliac bone in 38/70 (54.3%) of cases, lumbar vertebra in 10/70 (14.3%), thoracic vertebra in 7/70 (10%), sacrum in 4/70 (5.7%) and femur in 3/70 (4.3%). Two bone biopsies each (altogether 8.7%) were procured from pubic bone, rib and ischial bone, and 1/70 (1.5%) biopsy each was taken from sternum and humerus (Table 1). In seven of these biopsies, material was obtained from two anatomically distinct sites during the same procedure. In all seven cases, one biopsy was obtained from the iliac bone. The second biopsy was procured from the opposite iliac bone in three cases, from sacrum in two and from sternum and lumbar vertebra in one case each. All seven procedures with two biopsy sites – 14 total biopsies – yielded diagnostic material.

In 60/70 (85.7%) cases, tissue was procured using the Arrow® OnControl® Powered Bone Marrow Biopsy System. The Temno Evolution™ Biopsy Device (18G), the MADISON™ Comprehensive Bone Biopsy System and the Westcott Fine Needle Aspiration Biopsy (22G) were used in the remainder 5 (7.1%), 4 (5.7%) and 1 (1.4%) cases, respectively. No complications (e.g. clinically apparent hematoma or infection) were reported. One patient was found to have two sclerotic lesions in the right iliac bone. We performed an additional sodium fluoride (^{18}F-NaF) PET-MRI to identify the most metabolic active lesions.[14] Based on the results, the biopsy plan was subsequently adjusted to target L5 and anterior superior iliac spine (Figure 4).

Biopsy processing and histopathology

Sixty out of 70 (85.7%) tissue samples contained enough tumor tissue to establish a diagnosis, and the other 10 (14.3%) samples were non-diagnostic. Sufficient FFPE tissue was available to perform routine IHC in 33/60 (55.0%) cases. Pathology classification of positive biopsies demonstrated that 55/60 (91.7%) cases contained usual prostate adenocarcinoma histology[10] (Table 1).

Metrics for NGS

Tumor tissue was sufficient for sequencing in 49 (81.7%) of all 60 diagnostic cases. The tumor content was estimated by histopathology evaluation (data not shown) and by using an algorithm to assess tumor DNA purity and cancer cell ploidy (CLONET),[12] and ranged between 10%- 93.9% (mean CLONET tumor purity in bone biopsies: 49.6%, mean CLONET tumor purity in blood clots: 55.9%). No differences in DNA yield, tumor cell content, coverage and capture efficiency was observed between anatomic locations. Data on DNA concentration from the bone/blood clot samples were available for 46/60 (76.9%) samples. Median DNA concentration was overall 25.5ng/μl (range: 0.53-164.40 ng/μl), 41.4ng/μl for DNA from blood clots and 32.3ng/μl for DNA from bone biopsies (p=0.40). Median 260/280 ratio was 1.81 for DNA and 1.95 for RNA, thus sufficient for subsequent NGS. Whole-exome sequencing (WES), requiring minimum 225ng DNA, was successful in 49 of 60 diagnostic cases (81.7%).[9] Mean input was 232.72ng DNA for WES and 323.13ng RNA for RNAseq. WES was successfully performed from blood clots in 26/56 (46.5%) and from bone biopsies in 23/63 (36.5%) of cases. Mean capture efficiency was 83.6% and mean coverage was 94.7%. Recurrent alterations were as expected in metastatic prostate cancer and included mutation or amplification of the *AR* (4.0% mutation, 32.7% amplification) gene, deletion of *PTEN* (10.2%), mutation or deletion of *TP53* (14.3% mutation, 2% deletion), mutation or deletion of *BRCA2* (10.2% mutation, 4.0% deletion), and mutation of *SPOP* (4%) genes.[5]

In 37/60 (61.7%) of diagnostic cases, the amount of tissue was insufficient to perform concurrent DNA and RNA extraction, and WES was prioritized. There was enough tissue to run additionally RNA-seq in 23/60 diagnostic cases (requiring minimum 100ng RNA), of which RNA-seq was successfully performed in 20/23 (87.0%). Data on RNA concentration from the bone/blood clot samples were available for 11 samples. Median RNA concentration was overall 16.2ng/μl. The remaining three of 23 (13.0%) samples failed RNA-seq due to poor per base sequence quality (See Supplementary Table 1 for quality control metrics and additional results).

Discussion

Patients with advanced prostate cancer commonly harbor sclerotic bone metastases, which are challenging sites to biopsy and the tumor tissue obtained is often limited. We developed a protocol to successfully procure high-quality nucleic acids from metastatic tumors for sequencing, specifically from bone biopsy specimen. We focused on optimizing techniques that limit patient risk by limiting procedure time and radiation exposure and maximizing tissue samples such as the use of blood clots for successful NGS. We also wanted to develop a protocol not relying on time-consuming techniques such as laser capture microdissection, as these are not always available. We instead sampled cryomolds with a biopsy needle using the annotated H&E slide as guide; this technique resulted in a tumor purity sufficient for subsequent NGS in the vast majority of cases.

Percutaneous bone biopsies have a low complication rate, with a range in the literature from 0 to 7.4%[15]. Common complications include muscular hematomas and bleeding, and rarely biopsy device fracture, nerve injury, and cerebrospinal fluid leak.[16] No complications were

seen in our series, which correlates with other published series utilizing a drill-assisted biopsy system.[17] Fracture of a biopsy device in the thoracic spine has been reported with the use of a 16-gauge Bonopty® device.[16] In a series of 162 consecutive patients using the Bonopty® device, sclerotic lesions were significantly associated with a lower diagnostic yield.[18] This difference was not seen in our cohort: 85.2% and 87.7% of sclerotic and lytic lesions, respectively, were diagnostic (p=0.187). This is also a significantly higher rate of diagnostic biopsies than previously reported for CT-guided biopsies (Table 2, shows a comparison of our results with other published studies of bone biopsies in metastatic prostate cancer).[20, 21] In a series of 39 biopsies from patients with metastatic prostate cancer, 77% had at least one positive biopsy core. The authors found, that skin-to-bone distance <6.1 cm was associated with a higher tumor yield on biopsy.[20] In contrast, in our series we were able to successfully sequence 88.5% (23/26) of cases where skin-to-bone distance was >6.1 cm. We observed that the drill-assisted biopsy system improved the diagnostic yield, thus, there was no need to further stratify patients according to published radiologic and clinical criteria for selection, since the biopsy was likely to be diagnostic.[21] In one patient, additional ^{18}F-NaF PET-MRI was performed to evaluate two lesions in the iliac bone and biopsy site was subsequently adjusted.[14] PET-MRI has been shown to be more sensitive than PET-CT in detecting bone metastases.[22] It might be a valuable additional tool for identifying the lesion promising the greatest yield of tumor tissue.

To the best of our knowledge, this is the first publication that describes utilization of blood clots for NGS, which can be obtained through the drill-assisted biopsy systems. While cortical bone lesions may have to be decalcified, blood clots can be frozen and further utilized without additional processing.

Inadequate biopsies may subject the patient to risk without benefit. To date, little has been published assessing the quality of bone biopsies for NGS. One study found a sequencing failure rate of 5 out of 21 FFPE bone biopsies, the reason for this is uncertain due to lack of information about pre-analytical variables like decalcification.[7] In our study, the median DNA yield was sufficient for WES (requiring >225ng) in most cases and would also have been sufficient for other commonly used targeted gene panels (requiring 10-300ng).[23]

In seven patients, concurrent biopsies from two anatomically distinct sites were performed with an excellent diagnostic yield of 100% and subsequent successful WES in 5/7 (71.4%) cases. Performing double biopsies increased procedural time slightly, however, no complications were seen. This approach could be beneficial to increase the overall amount of tissue. The additional radiation exposure is negligible and could avoid additional biopsy procedures should the initial attempt fails to be diagnostic.

While liquid biopsies such as circulating tumor DNA (ctDNA) are attractive as non-invasive methods for molecular biomarker detection, metastatic tumor biopsies do provide additional information not currently captured well by liquid approaches. For instance, our approach is to ensure that bone biopsies – and blood clots when available – are handled in a way that allows for morphology assessment and also preserves RNA. Spritzer et al. report a 39% yield for RNA utilizing a 15G Bonopty® system. In their study, all five iliac bone biopsies in sites other than adjacent to the sacroiliac joint were insufficient for RNA isolation. In our

current study, 6/7 sclerotic lesions and 2/2 of lytic lesions in such sites were adequate for sequencing.

Conclusions

Historically, the goal of cancer biopsies has aligned with the concept of adequacy, or obtaining just enough sample to allow pathologists to confirm a diagnosis. It is now recognized that anti-neoplastic treatment changes the molecular landscape of metastatic tumors.[24, 25] Our experience highlights a necessary shift in paradigm in an era of Precision Medicine from adequate to sufficient biopsies to address both diagnostic and molecular needs. The results presented herein demonstrate that this can be performed safely, without significant complications.

Supplementary Material

Refer to Web version on PubMed Central for supplementary material.

Acknowledgments

This work was also supported by the Translational Research Program at WCM Pathology and Laboratory Medicine. The Englander IPM clinical team coordinated clinical activities. Rob Kim provided administrative support. Logistic support was provided by Elyze C. Merzier. Art design was provided by Rogério Paulo da Silva.

Research support: This research was supported by the US National Institutes of Health (NIH) R01 CA116337 (H.B. and M.A.R.), 5U01 CA111275-09 (J.M.M. and M.A.R.), Department of Defense PCRP PC121341 (H.B.), Starr Cancer Consortium (H.B. and M.A.R), Nuovo Soldati Foundation (J.C.).

References

1. Halabi S, Kelly WK, Ma H, et al. Meta-Analysis Evaluating the Impact of Site of Metastasis on Overall Survival in Men With Castration-Resistant Prostate Cancer. J Clin Oncol. 2016; 34:1652–1659. [PubMed: 26951312]
2. Bubendorf L, Schopfer A, Wagner U, et al. Metastatic patterns of prostate cancer: an autopsy study of 1,589 patients. Hum Pathol. 2000; 31:578–583. [PubMed: 10836297]
3. Siegel RL, Miller KD, Jemal A. Cancer Statistics, 2017. CA Cancer J Clin. 2017; 67:7–30. [PubMed: 28055103]
4. Mateo J, Carreira S, Sandhu S, et al. DNA-Repair Defects and Olaparib in Metastatic Prostate Cancer. N Engl J Med. 2015; 373:1697–1708. [PubMed: 26510020]
5. Robinson D, Van Allen EM, Wu YM, et al. Integrative clinical genomics of advanced prostate cancer. Cell. 2015; 161:1215–1228. [PubMed: 26000489]
6. Van Allen EM, Foye A, Wagle N, et al. Successful whole-exome sequencing from a prostate cancer bone metastasis biopsy. Prostate Cancer Prostatic Dis. 2014; 17:23–27. [PubMed: 24366412]
7. Zheng G, Lin MT, Lokhandwala PM, et al. Clinical mutational profiling of bone metastases of lung and colon carcinoma and malignant melanoma using next-generation sequencing. Cancer. 2016; 124:744–753.
8. Spritzer CE, Afonso PD, Vinson EN, et al. Bone marrow biopsy: RNA isolation with expression profiling in men with metastatic castration-resistant prostate cancer--factors affecting diagnostic success. Radiology. 2013; 269:816–823. [PubMed: 23925271]
9. Beltran H, Eng K, Mosquera JM, et al. Whole-Exome Sequencing of Metastatic Cancer and Biomarkers of Treatment Response. JAMA Oncol. 2015; 1:466–474. [PubMed: 26181256]
10. Epstein JI, Amin MB, Beltran H, et al. Proposed morphologic classification of prostate cancer with neuroendocrine differentiation. Am J Surg Pathol. 2014; 38:756–767. [PubMed: 24705311]

11. Mardis E, McCombie WR. Library Quantification: Fluorometric Quantitation of Double-Stranded or Single-Stranded DNA Samples Using the Qubit System. Cold Spring Harb Protoc. 2016
12. Prandi D, Baca SC, Romanel A, et al. Unraveling the clonal hierarchy of somatic genomic aberrations. Genome Biol. 2014; 15:439. [PubMed: 25160065]
13. Demichelis F, Greulich H, Macoska JA, et al. SNP panel identification assay (SPIA): a genetic-based assay for the identification of cell lines. Nucleic Acids Res. 2008; 36:2446–2456. [PubMed: 18304946]
14. Rakheja R, Chandarana H, Ponzo F, et al. Fluorodeoxyglucose positron emission tomography/magnetic resonance imaging: current status, future aspects. PET Clin. 2014; 9:237–252. [PubMed: 25030285]
15. Hau A, Kim I, Kattapuram S, et al. Accuracy of CT-guided biopsies in 359 patients with musculoskeletal lesions. Skeletal Radiol. 2002; 31:349–353. [PubMed: 12073119]
16. Shaikh H, Thawani J, Pukenas B. Needle-in-Needle Technique for Percutaneous Retrieval of a Fractured Biopsy Needle during CT-Guided Biopsy of the Thoracic Spine. Interv Neuroradiol. 2014; 20:646–649. [PubMed: 25363270]
17. Wallace AN, McWilliams SR, Wallace A, et al. Drill-Assisted Biopsy of the Axial and Appendicular Skeleton: Safety, Technical Success, and Diagnostic Efficacy. J Vasc Interv Radiol. 2016; 27:1618–1622. [PubMed: 27670996]
18. Li Y, Du Y, Luo TY, et al. Factors influencing diagnostic yield of CT-guided percutaneous core needle biopsy for bone lesions. Clin Radiol. 2014; 69:e43–47. [PubMed: 24268511]
19. Ross RW, Halabi S, Ou SS, et al. Predictors of prostate cancer tissue acquisition by an undirected core bone marrow biopsy in metastatic castration-resistant prostate cancer--a Cancer and Leukemia Group B study. Clin Cancer Res. 2005; 11:8109–8113. [PubMed: 16299243]
20. McKay RR, Zukotynski KA, Werner L, et al. Imaging, procedural and clinical variables associated with tumor yield on bone biopsy in metastatic castration-resistant prostate cancer. Prostate Cancer Prostatic Dis. 2014; 17:325–331. [PubMed: 25091040]
21. Lorente D, Omlin A, Zafeiriou Z, et al. Castration-Resistant Prostate Cancer Tissue Acquisition From Bone Metastases for Molecular Analyses. Clin Genitourin Cancer. 2016; 14:485–493. [PubMed: 27246360]
22. Catalano OA, Nicolai E, Rosen BR, et al. Comparison of CE-FDG-PET/CT with CE-FDG-PET/MR in the evaluation of osseous metastases in breast cancer patients. Br J Cancer. 2015; 112:1452–1460. [PubMed: 25871331]
23. Chen H, Luthra R, Goswami RS, Singh RR, Roy-Chowdhuri S. Analysis of Pre-Analytic Factors Affecting the Success of Clinical Next-Generation Sequencing of Solid Organ Malignancies. Cancers (Basel). 2015; 7:1699–1715. [PubMed: 26343728]
24. Pao W, Miller VA, Politi KA, et al. Acquired resistance of lung adenocarcinomas to gefitinib or erlotinib is associated with a second mutation in the EGFR kinase domain. PLoS Med. 2005; 2:e73. [PubMed: 15737014]
25. Cancer Genome Atlas Research N. The Molecular Taxonomy of Primary Prostate Cancer. Cell. 2015; 163:1011–1025. [PubMed: 26544944]

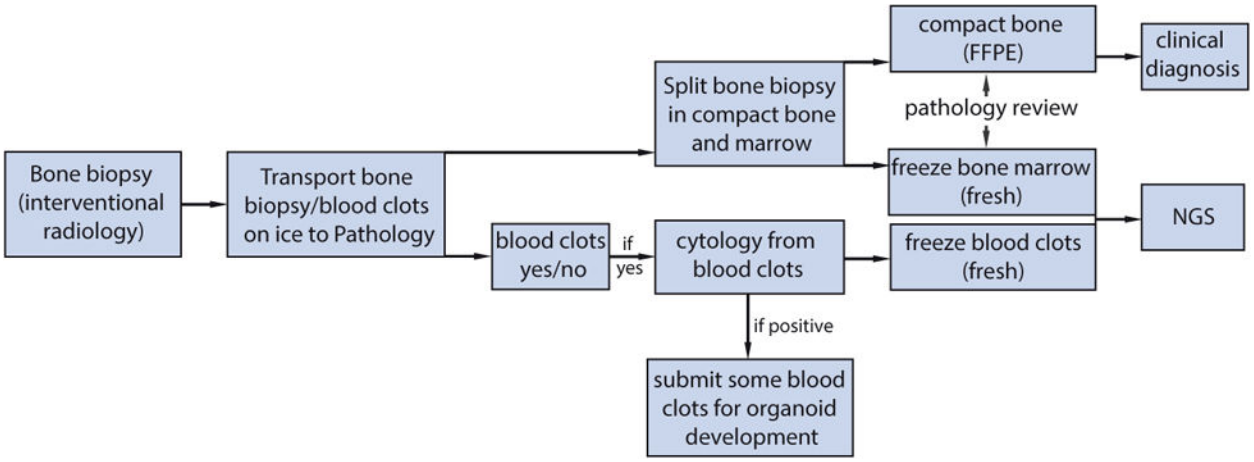

Figure 1.

Proposed next-generation bone biopsy protocol in metastatic prostate cancer. Schematic illustration of the biopsy workflow is shown. See additional details in Supporting Information Table 1. FFPE indicates formalin-fixed, paraffin-embedded; NGS, next-generation sequencing.

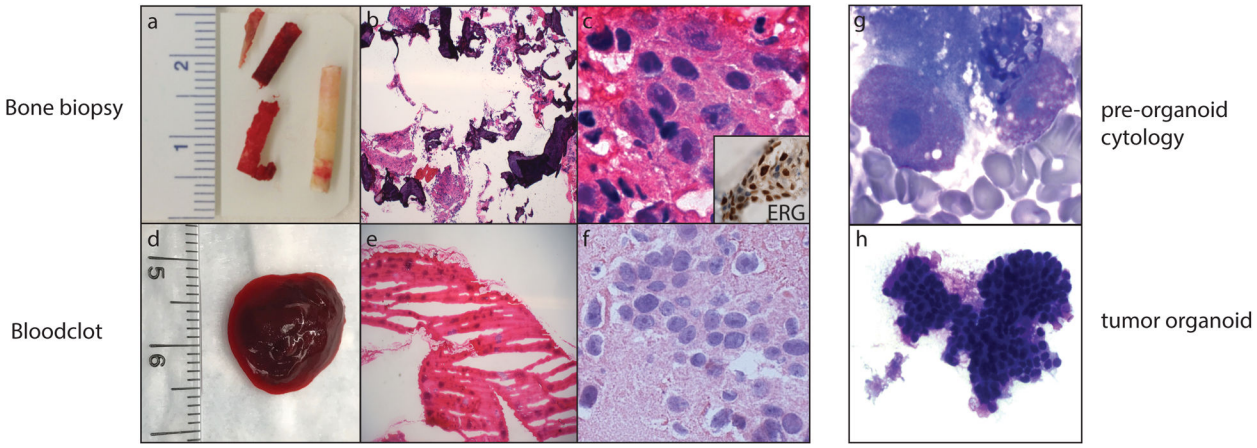

Figure 2.

Bone biopsy material used for diagnosis, next-generation sequencing (NGS), and preclinical models. (a) Macroscopic image of a bone biopsy. Compact bone (whitish core) and bone marrow (reddish core) are split upon receipt, and submitted for clinical diagnosis and NGS, respectively. (b and c) Histology of metastatic prostate adenocarcinoma using images from corresponding frozen bone marrow (H & E; low and high magnification). *Inset*: ETS-related gene (ERG)-positive immunohistochemistry in tumor cells. (d) Macroscopic image of a fresh blood clot. (e and f) Histology of metastatic prostate adenocarcinoma using images from a corresponding frozen blood clot (H & E; low and high magnification). (g) Adequacy and tumor cell content are evaluated by cytologic smear examination of the biopsy and/or blood clot (Diff-Quik). (h) Morphologic evaluation of organoid in culture by cytologic smear examination (Diff-Quik).

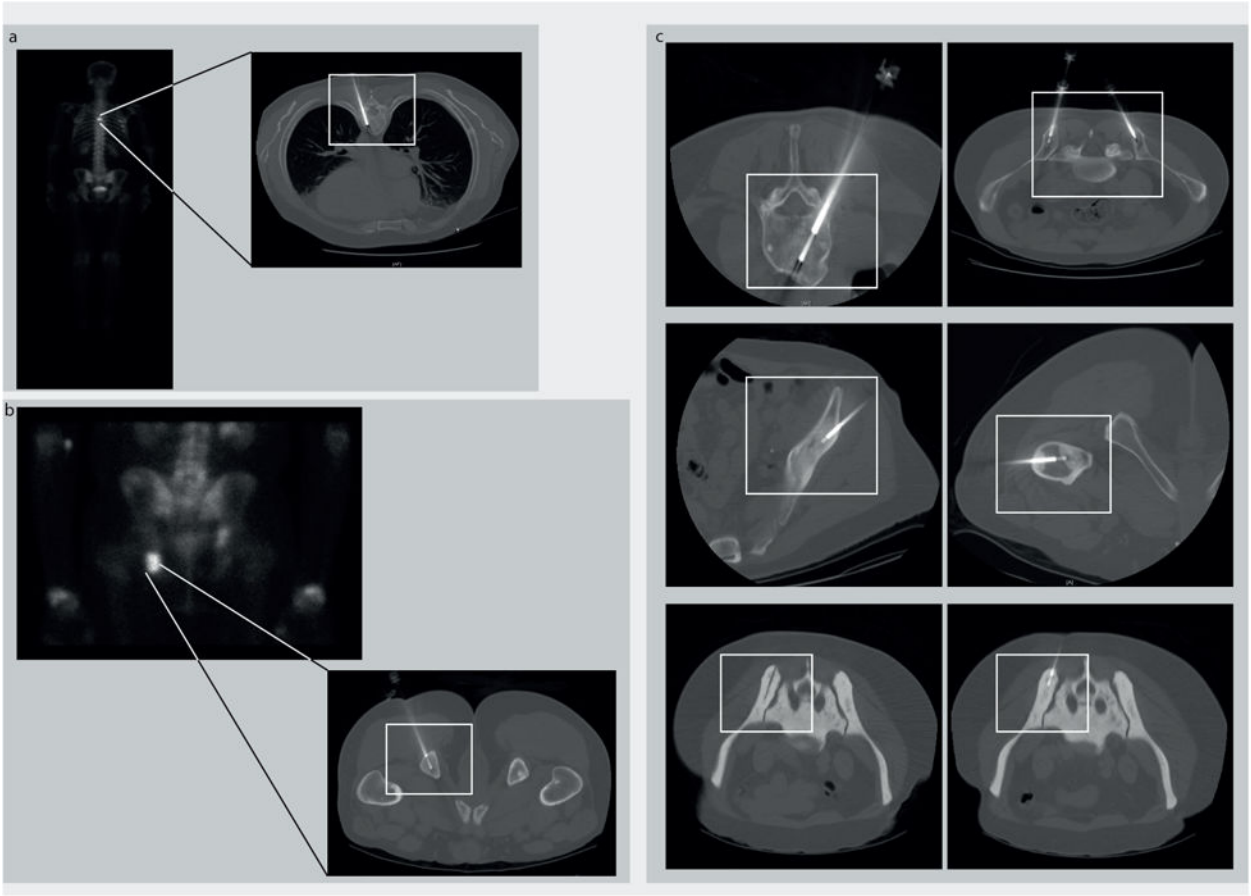

Figure 3.

Radiology images of different bone lesions in patients with metastatic prostate cancer who underwent a biopsy using the OnControl drill. (a) T6 vertebral body lesion and (b) lesion of the left ischial tuberosity. (*Left*) Scintigraphic image with clearly visible tracer uptake in both lesions. (*Right*) A corresponding computed tomography (CT) image demonstrating the intralesional biopsy needle. (c) CT images of biopsy procedures in multiple locations in several patients demonstrating safe use of the OnControl drill throughout the bony skeleton. CT-guided biopsy of an extremely dense bone lesion (lower panels: white rectangle, OnControl). The CT images confirm a technically successful biopsy.

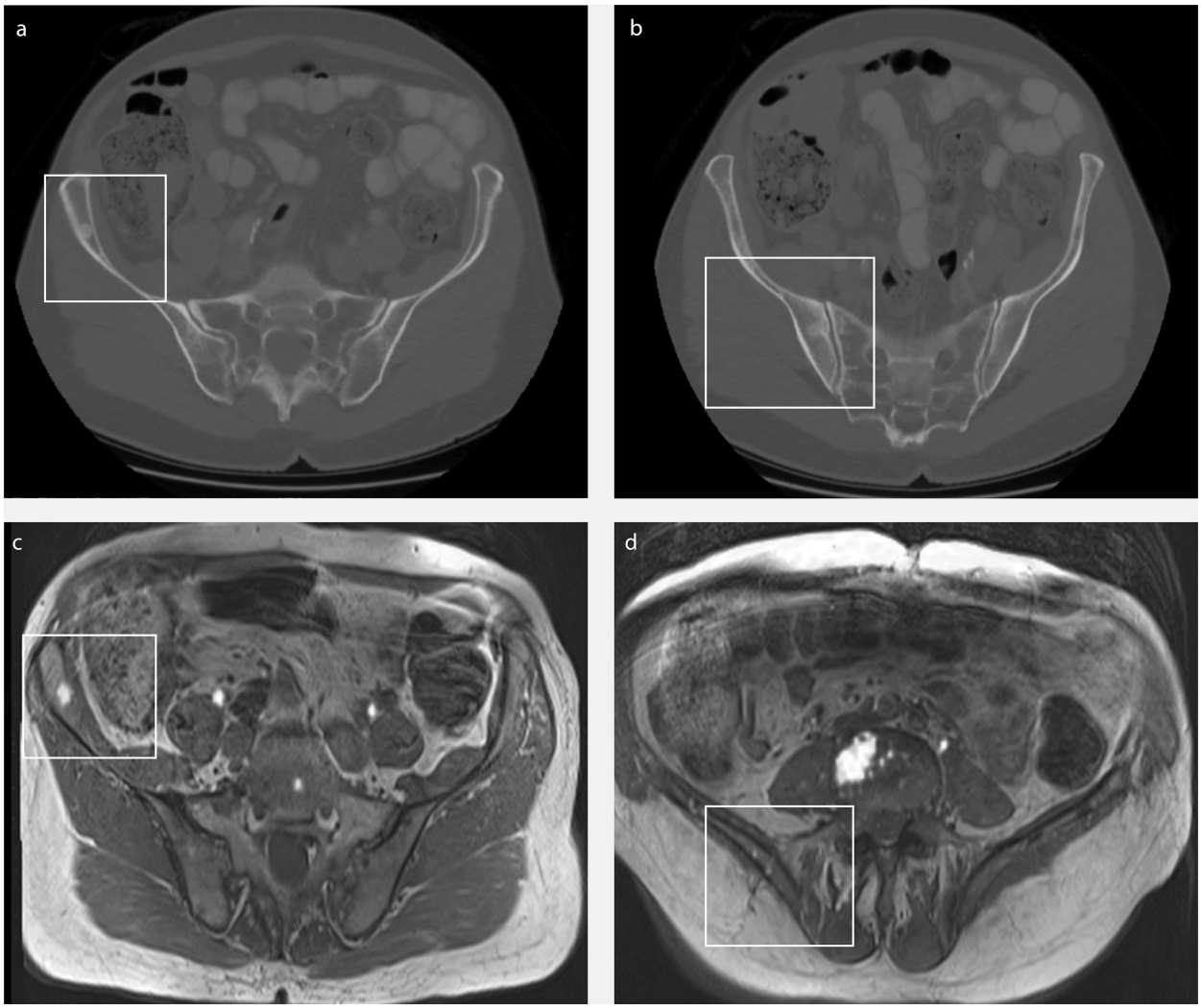

Figure 4.

Addition of positron emission tomography (PET)-magnetic resonance imaging (MRI) to help identify which lesion to biopsy. (a and b) A 73-year-old patient with 2 bone lesions in the right iliac bone (white rectangle) shown on computed tomography. 18 F-sodium fluoride (18F-NaF) PET-MRI clearly identified (c) tracer enrichment in the anterior lesion, (d) with no enrichment noted in the posterior lesion. The biopsy plan subsequently was changed to target the anterior lesion and the L5 vertebra.

Biopsies from patients with prostate cancer bone metastases can provide high-quality tissue for next-generation sequencing. The authors believe the protocol described in the current study is widely applicable to all bone metastases.

Table 1
Clinical and Pathological Characteristics of 70 Bone Metastases From 64 Patients

Characteristic	No [%]
Number of procedures	70 [100]
Age, years	
Mean	70.3 + 8.7
Median	71
Radiologic appearance of bone metastasis	
Blastic	61 [87.1]
Lytic	8 [11.4]
Mixed	1 [1.4]
Location	
Iliac bone	38 [54.3]
Lumbar vertebra	10 [14.3]
Thoracic vertebra	7 [10.0]
Sacrum	4 [5.7]
Femur	3 [4.3]
Pubic bone	2 [2.9]
Rib	2 [2.9]
Ischiac bone	2 [2.9]
Sternum	1 [1.4]
Humerus	1 [1.4]
Biopsy diagnostic	
Yes	60 [85.7]
No	10 [14.3]
Histologic subtype[(a)]	
Adenocarcinoma, usual	55 [91.7]
Adenocarcinoma, with neuroendocrine differentiation	3 [5.0]
Small cell carcinoma	2 [3.3]

[(a)] Percentages based on 60 diagnostic biopsies

Table 2

Comparison of Results of the Current Study With Other Published

No of procedures	Image guidance?	Diagnostic yield	Sufficiency for molecular studies	Reference	PMID
80	Yes	69%	64%	Holmes et al.	28549709
54	Yes	67%	39%	Spritzer et al.	23925271
115	No	65.2%	not performed	Lorente et al.	27246360
39	Yes	77%	not performed	McKay et al.	25091040
70	Yes	85.7%	81.7%	This study	N/A